1.17

DIFFUSION AND CONFIGURATIONAL DISORDER IN MULTICOMPONENT SOLIDS

A. Van der Ven and G. Ceder
Department of Materials Science and Engineering, Massachusetts Institute of Technology, Cambridge, MA, USA

1. Introduction

Atomic diffusion in solids is a kinetic property that affects the rates of important nonequilibrium phenomena in materials. The kinetics of atomic redistribution in response to concentration gradients determine not only the speed, but often also the mechanism by which phase transformations in multicomponent solids occur. In electrode materials for batteries and fuel cells high mobilities of specific ions ranging from lithium or sodium to oxygen or hydrogen are essential. In many instances, diffusion occurs in nondilute regimes in which different migrating atoms interact with each other. For example, lithium intercalation compounds such as Li_xCoO_2 and Li_xC_6 which serve as electrodes in lithium-ion batteries, can undergo large variations in lithium concentrations, ranging from very dilute concentrations to complete filling of all interstitial sites available for Li in the host. In nondilute regimes, diffusing atoms interact with each other, both electronically and elastically. A complete theory of nondilute diffusion in multi-component solids needs to account for the dependence of the energy and migration barriers on the configuration of diffusing ions.

In this chapter, we present the formalism to describe and model diffusion in multicomponent solids. With tools from alloy theory to describe configurational thermodynamics [1–3], it is now possible to rigorously calculate diffusion coefficients in nondilute alloys from first-principles. The approach relies on the use of the alloy cluster expansion which has proven to be an invaluable statistical mechanical tool that links first-principles energies to the thermodynamic and kinetic properties of solids with configurational disorder. Although diffusion is a nonequilibrium phenomenon, diffusion coefficients

S. Yip (ed.),
Handbook of Materials Modeling, 367–394.

can nevertheless be calculated by considering fluctuations at equilibrium using Green–Kubo relations [4].

We first elaborate on the atomistic mechanisms of diffusion in solids with interacting diffusing species. This is followed with a discussion of the relevant Green–Kubo expressions for diffusion coefficients. We then introduce the cluster expansion formalism to describe the configurational energy of a multi-component solid. We conclude with several examples of first-principles calculations of diffusion coefficients in multi-component solids.

2. Migration in Solids with Configurational Disorder

Multi-component crystalline solids under most thermodynamic boundary conditions are characterized by a certain degree of configurational disorder. The most extreme example of configurational disorder occurs in a solid solution in which on average the arrangements of the different components of the solid approximate randomness. But even ordered compounds exhibit some degree of disorder due to thermal excitations or slight off-stoichiometry of the bulk composition. Atoms diffusing over crystal sites of a disordered solid sample a variety of different local environments along their trajectory.

Diffusion in most crystals can be characterized as a Markov process whereby atoms after each hop completely thermalize before migrating to the next site along its trajectory. Hence each hop is independent of all previous hops. With reasonable accuracy, the rate with which individual atomic hops occur, can be described with transition state theory according to

$$\Gamma = \nu^* \exp\left(\frac{-\Delta E_b}{k_B T}\right) \tag{1}$$

where ν^* is a vibrational prefactor (having units of Hz) and ΔE_b is an activation barrier. Within the harmonic approximation, the vibrational prefactor is a ratio between the vibrational eigenmodes of the solid at the initial state of the hop to the vibrational eigenmodes when the migrating atom is at the activated state [5].

In the presence of configurational disorder, the activation barrier and frequency prefactor depend on the local arrangement of atoms around the migrating atom. Modeling of diffusion in a multicomponent system therefore requires a knowledge of the dependence of ΔE_b and ν^* on configuration. Especially, the configuration dependence of ΔE_b is of importance as the hop frequency, Γ, depends on it exponentially.

We restrict ourselves here to migration that occurs by individual atomic hops to adjacent *vacant* sites. Hence we do not consider diffusion that occurs through either a *ring* or *intersticialicy* mechanism. We also make a distinction between diffusion of interstitial species and substitutional species.

2.1. Interstitial Diffusion

Interstitial diffusion occurs in many important materials. A common example is the diffusion of carbon atoms over the interstitial sites of bcc or fcc iron (i.e., steel). Many phase transformations in steel involve the redistribution of carbon atoms between growing precipitate phases and the consumed matrix phase. A defining characteristic of interstitial diffusion is the existence of an externally imposed lattice of sites over which atoms can diffuse. In steel, the crystallized iron atoms create the interstitial sites for carbon. A similar situation exists in Li_xCoO_2 in which a crystalline CoO_2 host creates an array of intersitial sites that can be occupied by lithium. While in Li_xCoO_2, the lithium concentration x can be varied from 0 to 1, in steel FeC_y, the carbon concentration y is typically very low. Individual carbon atoms interfere minimally with each other as they wander over the interstitial sites of iron. In Li_xCoO_2, however, as the lithium concentration is typically large, migrating lithium atoms interact strongly with each other and influence each other's diffusive trajectories.

Another type of system that we place in the category of interstitial diffusion is adatom diffusion on the surface of a crystalline substrate. Often a crystalline surface creates an array of well defined sites on which adsorbed atoms reside, such as the fcc sites on a (111) terminated surface of an fcc crystal. Diffusion then involves the migration of adsorbed atoms over these surface sites.

The presence of many diffusing atoms creates a state of configurational disorder over the interstitial sites that evolves over time as a result of the activated hops of individual atoms. Not only does the activation barrier of a migrating atom depend on the local arrangement of the surrounding interstitial atoms, but also the migration mechanism can depend on that arrangement. This is the case in Li_xCoO_2, a layered compound consisting of close packed oxygen planes stacked with an ABCABC sequence. Between the oxygen layers are alternating layers of Li and Co which occupy octahedral sites of the oxygen sublattice. Within each lithium plane, the lithium ions occupy a two dimensional triangular lattice. As lithium is removed from $LiCoO_2$, vacancies are created in the lithium planes. First-principles density functional theory calculations (LDA) have shown that two migration mechanisms for lithium exchange with an adjacent vacancy exist depending on the arrangement of surrounding lithium atoms [3]. This is illustrated in Fig. 1. If the two sites adjacent to the end points of the hop (sites (a) and (b) in Fig. 1a) are simultaneously occupied by lithium ions, then the migration mechanism follows a direct path, passing through a dumbel of oxygen atoms. The calculated activation barrier for this mechanism is high, approaching 0.8 eV. This mechanism occurs when lithium migrates to an isolated vacancy. If, however, one or both of the sites adjacent to the end points of the hop are vacant (Fig. 1b), then the migrating lithium follows a curved path which passes through an adjacent tetrahedral

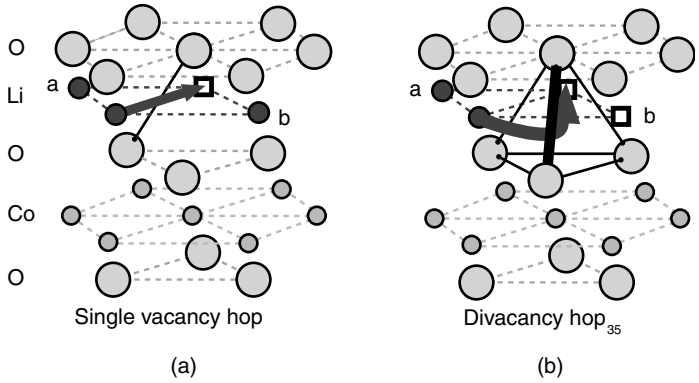

Figure 1. Two lithium migration mechanims in Li_xCoO_2 depending on the arrangement of lithium ions around the migrating ion. (a) When both sites *a* and *b* are occupied by Li, the migrating lithium performs a direct hop whereby it has to squeeze through a dumbel of oxygen ions. This mechanism occurs when the migrating lithium ion hops into an isolated vacancy (square). (b) When either site *a* or site *b* are vacant, the migrating lithium ion performs a curved hop whereby it passes through a tetrahedrally coordinated site. This mechanism occurs when the migrating atom hops into a divacancy.

site, out of the plane formed by the Li sites. For this mechanism, the activation barrier is low, taking values in the vicinity of 0.3–0.4 eV. This mechanism occurs when lithium migrates into a divacancy. Comparison of the activation barriers for the two mechanisms clearly shows that lithium diffusion mediated with divacancies is more rapid than with single vacancies. Nevertheless, we can already anticipate that the availability of divacancies will depend on the overall lithium concentration.

The complexity of diffusion in a disordered solid is evident in Fig. 2 which schematically illustrates a typical disordered arrangement of lithium atoms within a lithium plane of Li_xCoO_2. Hop 1, for example, must occur with a large activation barrier as the lithium is migrating to an isolated vacancy. In hop 2, lithium migrates to a vacant site that belongs to a divacancy and hence follows a curved path passing through an adjacent tetrahedral site characterized by a low activation barrier. In hop 3, lithium migrates to a vacant site belonging to two divacancies simultaneously, and hence has two low energy paths available. Similar complexities can be expected for adatom diffusion on crystalline substrates.

2.2. Substitutional Diffusion

Substitutional diffusion is qualitatively different from interstitial diffusion in that an externally imposed lattice of sites for the diffusing atoms is absent.

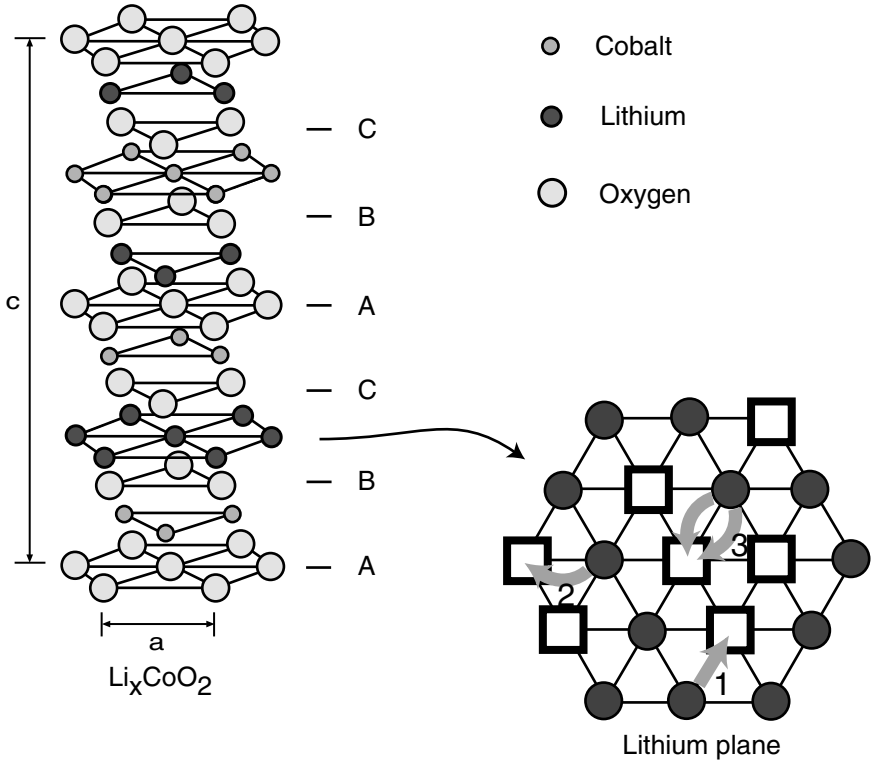

Figure 2. A typical disordered lithium-vacancy arrangement within the lithium planes of Li_xCoO_2. In a given lithium-vacancy arrangement, several different migration mechanisms can occur.

Instead, the diffusing atoms themselves form the network of crystal sites. This describes the situation for most metallic and semiconductor alloys. Vacancies with which to exchange with do exist in these crystalline alloys, however, the concentrations are often very dilute. Examples where substitutional diffusion is relevant are alloys such as Si–Ge, Al–Ti and Al–Li, in which the different species reside on the same crystal structure, and migrate by exchanging with vacancies.

As with intersitial compounds, widely varying degrees of local order or disorder exist, affecting migration barriers. $Al_{(1-x)}Li_x$ for example is metastable on the fcc crystal structure for low x and forms an ordered $L1_2$ compound at $x = 0.25$. Diffusion within a solid solution is different than in the ordered compound as the local arrangement of Li and Al are different. Figure 3 illustrates a diffusive hop of an Al atom to a neighboring vacancy within the ordered $L1_2$ Al_3Li phase. The energy along the migration path as calculated with LDA is also

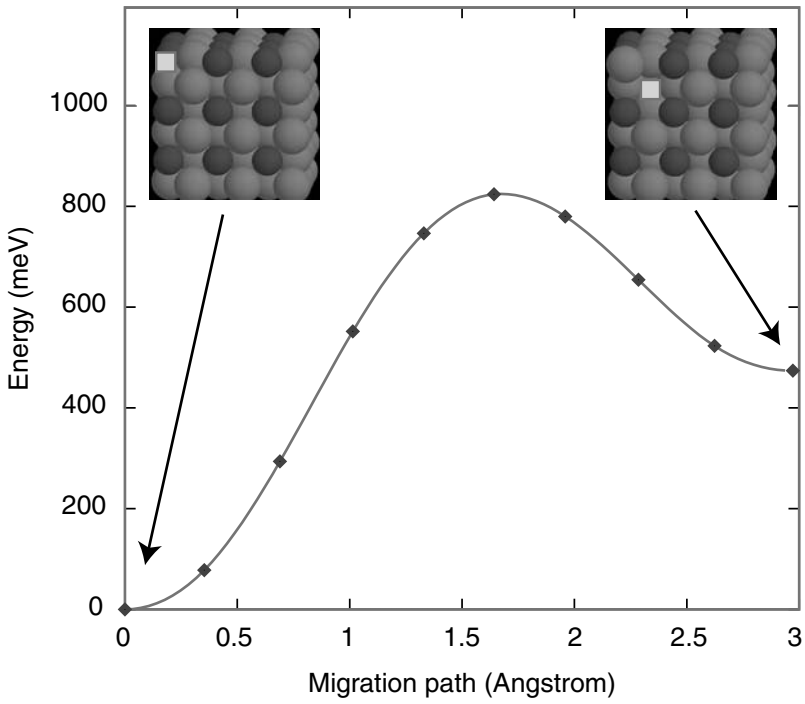

Figure 3. The energy along the migration path of an Al atom hopping into a vacancy (square) on the lithium sublattice of $L1_2$ Al_3Li. Lighter atoms are Al, darker atoms are Li.

illustrated in Fig. 3. Clearly, the vacancy prefers the Li sublattice as the energy of the solid increases as the vacancy migrates from the Li sublattice to the Al sublattice by exchanging with an Al atom.

3. Green–Kubo Expressions for Diffusion

While diffusion is complex at the atomic length scale, of central importance at the macroscopic length scale is the rate with which gradients in concentration dissipate. These rates can be described by diffusion coefficients that relate atomic fluxes to gradients in concentration. Green–Kubo methods make it possible to link kinetic coefficients to microscopic fluctuations of appropriate quantities at equilibrium. In this section we present the relevant Green–Kubo equations that allow us to calculate diffusion coefficients in multi-component solids from first-principles. We again make a distinction between interstitial and substitutional diffusers.

3.1. Interstitial Diffusion

3.1.1. Single component diffusion

For a single component occuping interstitial sites of a host, such as carbon in iron, or Li in Li_xCoO_2, irreversible thermodynamics [4] stipulates that a net flux J in particles occurs when a gradient in the chemical potential μ of the interstitial specie exists according to

$$J = -L\nabla\mu \tag{2}$$

where L is a kinetic coefficient that depends on the mobility of the diffusing atoms. Often it is more practical to express the flux in terms of a concentration gradient instead of a chemical potential gradient as the former is more accessible experimentally

$$J = -D\nabla C. \tag{3}$$

D in Eq. (3) is the diffusion coefficient and the concentration C refers to the number of interstitial particles per unit volume. While the true driving force for diffusion is a gradient in chemical potential, it is nevertheless possible to work with Eq. (3) provided the diffusion coefficient is expressed as

$$D = L\left(\frac{\mathrm{d}\mu}{\mathrm{d}C}\right). \tag{4}$$

Hence the diffusion coefficient consists of a kinetic factor L and a thermodynamic factor $\mathrm{d}\mu/\mathrm{d}C$.

The validity of irreversible thermodynamics is restricted to systems that are not too far removed from equilibrium. To quantify this, it is useful to mentally divide the solid into small subregions that are microscopically large enough for thermodynamic variables to be meaningful yet macroscopically small enough that the same thermodynamic quantities can be considered constant within each subregion. Hence, although the solid itself is removed from equilibrium, each subregion is locally at equilbrium. This is called the *local equilibrium* approximation, and it is within this approximation that the linear kinetic equation Eq. (2) is considered valid.

Within the local equilibrium approximation, the kinetic parameters D and L can be derived by a consideration of relevant fluctuations at thermodynamic equilibrium. Crucial in this derivation, is the assumption made by Onsager in his proof of the reciprocity relations of kinetic parameters, that the regression of a fluctuation of a particular extensive property around its equilibrium value occurs on average according to the same linear phenomenological laws as those governing the regression of artificially induced fluxes of the same extensive quantity [4]. This regression hypothesis is a consequence of the fluctuation–dissipation theorem of nonequilibrium statistical mechanics [6].

Several techniques, collectively referred to as Green–Kubo methods, exist to link microscopic fluctuations to macroscopic kinetic quantities [7–9]. Neglecting crystallographic anisotropy, the Green–Kubo expression for the kinetic factor for diffusion can be written as [10–12]

$$L = \frac{\left\langle \left(\sum_{\zeta} \Delta \vec{R}_{\zeta}(t) \right)^2 \right\rangle}{(2d)tMv_s k_B T} \tag{5}$$

where $\Delta \vec{R}_{\zeta}(t)$ is the vector connecting the end points of the trajectory of particle ζ after a time t, M refers to the total number of interstitial sites available, v_s is the volume per interstitial site, k_B is the Boltzmann constant, T is the temperature and d refers to the dimension of the interstitial network. The brackets indicate an ensemble average performed at equilibrium.

Often, the diffusion coefficient is also written in an equivalent form as [10]

$$D = D_J F \tag{6}$$

where

$$D_J = \frac{\left\langle \left(\sum_{\zeta} \Delta \vec{R}_{\zeta}(t) \right)^2 \right\rangle}{(2d)tN} \tag{7}$$

and

$$F = \frac{\mathrm{d}\left(\frac{\mu}{k_B T}\right)}{\mathrm{d}\ln(x)}. \tag{8}$$

N refers to the number of diffusing atoms and $x = N/M$ to the fraction of filled interstitial sites. F is often called a thermodynamic factor and D_J is sometimes called the jump-diffusion or self-diffusion coefficient.

A common approximation is to neglect cross correlations between different diffusing species and to replace D_J with the tracer diffusion coefficient defined as

$$D^* = \frac{\left\langle \Delta \vec{R}_{\zeta}^2(t) \right\rangle}{(2d)t}. \tag{9}$$

The difference between D_J and D^* is that the former depends on the square of the displacement of all the particles while the latter depends on the average of the square of the displacement of individual diffusing atoms. D_J is a measure of collective fluctuations of the center of mass of all the diffusing particles. Figure 4 compares D_J and D^* calculated with kinetic Monte Carlo simulations for the Li_xCoO_2 system. Notice in Fig. 4 that D_J is systematically larger than D^* for all lithium concentrations x, only approaching D^* for dilute lithium concentrations.

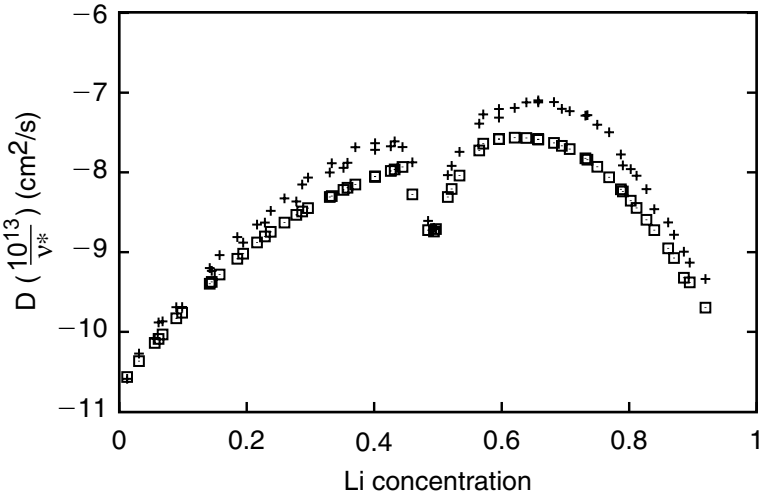

Figure 4. A comparison of the self diffusion coefficient D_J (crosses), and the tracer diffusion coefficient D^* (squares), for lithium diffusion in Li_xCoO_2 calculated at 400 K.

For interstitial components, the chemical potential of the diffusing atoms is defined as

$$\mu = \frac{dG}{dN} = \frac{dg}{dx} \tag{10}$$

where G is the free energy of the crystal containing the interstitial species and g is the free energy normalized per interstitial site. While the thermodynamic factor is related to the chemical potential according Eq. (8) it is often convenient to determine F by considering fluctuations in the number of interstitial atoms within the grand canonical ensemble (constant μ, T and M).

$$F = \frac{N}{\langle N^2 \rangle - \langle N \rangle^2} \tag{11}$$

Diffusion involves redistribution of particles from subregions of the solid with a high concentration of interstitial atoms to other subregions with a low concentration. The thermodynamic factor describes the thermodynamic response to concentration fluctuations within sub-regions.

3.1.2. Two component system

A similar formalism emerges when two different species reside and diffuse over the same interstitial sites of a host. This is the case for example for carbon and nitrogen diffusion in iron or lithium and sodium diffusion over the

interstitial sites of a transition metal oxide host. Referring to the two diffusing species as A and B, the flux equations become

$$J_{\mathrm{A}} = -L_{\mathrm{AA}}\nabla\mu_{\mathrm{A}} - L_{\mathrm{AB}}\nabla\mu_{\mathrm{B}} \qquad (12)$$
$$J_{\mathrm{B}} = -L_{\mathrm{BA}}\nabla\mu_{\mathrm{A}} - L_{\mathrm{BB}}\nabla\mu_{\mathrm{B}}$$

where L_{ij} (i, j = A or B) are kinetic coefficients similar to L of Eq. (2). As with Eq. (2), gradients in chemical potential are often not readily accessible experimentally and Eq. (12) can be written as

$$J_{\mathrm{A}} = -D_{\mathrm{AA}}\nabla C_{\mathrm{A}} - D_{\mathrm{AB}}\nabla C_{\mathrm{B}} \qquad (13)$$
$$J_{\mathrm{B}} = -D_{\mathrm{BA}}\nabla C_{\mathrm{A}} - D_{\mathrm{BB}}\nabla C_{\mathrm{B}}.$$

where the matrix of diffusion coefficients

$$\begin{pmatrix} D_{AA} & D_{AB} \\ D_{BA} & D_{BB} \end{pmatrix} = \begin{pmatrix} L_{AA} & L_{AB} \\ L_{BA} & L_{BB} \end{pmatrix} \begin{pmatrix} \dfrac{\partial\mu_A}{\partial C_A} & \dfrac{\partial\mu_A}{\partial C_B} \\ \dfrac{\partial\mu_B}{\partial C_A} & \dfrac{\partial\mu_B}{\partial C_B} \end{pmatrix} \qquad (14)$$

can again be factorized into a product of a kinetic term (the 2×2 $\mathbf{L}$ matrix) and a thermodynamic factor (the 2×2 matrix of partial derivative of the chemical potentials).

The Green–Kubo expressions relating the macroscopic diffusion coefficients to atomic fluctuations are [13, 14]

$$L_{ij} = \frac{\left\langle \left(\sum_\zeta \Delta\vec{R}^i_\zeta(t)\right)\left(\sum_\xi \Delta\vec{R}^j_\xi(t)\right)\right\rangle}{(2d)t v_{\mathrm{s}} M k_{\mathrm{B}} T}. \qquad (15)$$

where $\Delta\vec{R}^i_\zeta$ is the vector linking the end points of the trajectory of atom ζ of specie i after time t.

Another factorization of $\mathbf{D}$ is practical when studying diffusion with a lattice model description of the interactions between the different constituents residing on the crystal network

$$\mathbf{D} = \tilde{\mathbf{L}}\tilde{\boldsymbol{\Theta}} \qquad (16)$$

where

$$\tilde{L}_{ij} = \frac{\left\langle \left(\sum_\zeta \Delta\vec{R}^i_\zeta(t)\right)\left(\sum_\xi \Delta\vec{R}^j_\xi(t)\right)\right\rangle}{(2d)tM}. \qquad (17)$$

and

$$\tilde{\Theta}_{ij} = \frac{\partial\left(\frac{\mu_i}{k_B T}\right)}{\partial x_j}. \tag{18}$$

are respectively matrices of kinetic coefficients and thermodynamic factors.

As with the single component intersitial systems the chemical potentials for a binary component interstitial system are defined as

$$\mu_i = \frac{\partial G}{\partial N_i} = \frac{\partial g}{\partial x_i} \tag{19}$$

where i refers to either A or B. The components of $\tilde{\Theta}$ can also be written in terms of variances of the number of particles residing on the M site crystal network at constant chemical potentials, that is in terms of measures of fluctuations

$$\tilde{\Theta} = \frac{M}{Q}\begin{pmatrix} \langle N_B^2\rangle - \langle N_B\rangle^2 & -(\langle N_A N_B\rangle - \langle N_A\rangle\langle N_B\rangle) \\ -(\langle N_B N_A\rangle - \langle N_A\rangle\langle N_B\rangle) & \langle N_A^2\rangle - \langle N_A\rangle^2 \end{pmatrix} \tag{20}$$

where

$$Q = \left(\left\langle N_{\mathrm{A}}^2\right\rangle - \langle N_{\mathrm{A}}\rangle^2\right)\left(\left\langle N_{\mathrm{B}}^2\right\rangle - \langle N_{\mathrm{B}}\rangle^2\right) - (\langle N_{\mathrm{A}} N_{\mathrm{B}}\rangle - \langle N_{\mathrm{A}}\rangle\langle N_{\mathrm{B}}\rangle)^2$$

These fluctuations in N_{A} and N_{B} are to be calculated in the grand canonical ensemble at the chemical potentials μ_{A} and μ_{B} corresponding to the concentrations at which the diffusion coefficient is desired.

3.2. Substitutional Diffusion

The starting point for treating substitutional diffusion in a binary alloy are the Green–Kubo relations of Eqs. (14)–(18). However, several modifications and qualifications are necessary. These arise from the fact that alloys are characterized by a dilute concentration of vacancies and that the crystallographic sites on which the diffusing atoms reside are not created externally by a host, but are rather formed by the diffusing atoms themselves. The consequences of this for diffusion is that the chemical potentials appearing in the thermodynamic factor are not the conventional chemical potentials for the individual species A and B of a substitutional alloy, but are rather differences in chemical potentials between that of each diffusing specie and the vacancy chemical potential. Hence the chemical potentials of Eqs. (12), (14) and (18) need to be replaced by $\tilde{\mu}_i$ in which

$$\tilde{\mu}_i = \mu_i - \mu_{\mathrm{V}} \tag{21}$$

where μ_V is the vacancy chemical potential in the solid. The reason for this modification arises from the fact that the chemical potential appearing in the Green–Kubo expression for the diffusion coefficient matrix Eq. (14) and defined in Eq. (19) corresponds to the change in free energy as component i is added by holding the number of crystalline sites constant, meaning that i is added at the *expense of vacancies*. This differs from the conventional chemical potentials of alloys which are defined as the change in free energy of the solid as component i is added by extending the crystalline network of the solid. $\tilde{\mu}_i$ refers to the chemical potential for a fixed crystalline network, while μ_i and μ_V correspond to chemical potentials for a solid in which the crystalline network is enlarged as more species are added.

The use of $\tilde{\mu}_i$ instead of μ_i in the thermodynamic factor of the Green–Kubo expressions for the diffusion coefficients of crystalline solids also follows from irreversible thermodynamics [15, 16] as well as thermodynamic considerations of crystalline solids [17]. It can also be understood on physical grounds. By dividing the crystalline solid up into subregions, diffusion can be viewed as the flow of particles from one subregion to the next. Because of the constraint imposed by the crystalline network, the only way for excess atoms from one sub-region to be accommodated by a neighboring subregion is through the exchange of vacancies. One subregion gains vacancies the other loses them. The change in free energy in each subregion due to diffusion occurs by adding or removing atoms at the expense of vacancies.

Another important modification to the treatment of binary interstitial diffusion is the identification of interdiffusion. Interdiffusion in its most explicit form refers to the dissipation of concentration gradients by the intermixing of A and B atoms. It is this phenomenon of intermixing that enters into continuum descriptions of diffusion couples and phase transformations involving atomic redistribution.

Kehr *et al.* [18] demonstrated that in the limit of dilute vacancy concentrations, the full 2×2 diffusion matrix can be diagonalized producing an eigenvalue λ^+ corresponding to density relaxations due to inhomegeneities in vacancies and an eigenvalue λ^- corresponding to interdiffusion. The diagonalization of the $\mathbf{D}$ matrix is accompanied by a coordinate transformation of the fluxes and the concentration gradients. In matrix notation,

$$\mathbf{J} = -\mathbf{D}\nabla\mathbf{C} \tag{22}$$

where $\mathbf{J}$ and $\nabla\mathbf{C}$ are column vectors containing as elements J_A, J_B and ∇C_A, ∇C_B, respectively. Diagonalization of $\mathbf{D}$ leads to

$$\mathbf{D} = \mathbf{E}\lambda\mathbf{E}^{-1} \tag{23}$$

where $\boldsymbol{\lambda}$ is a diagonal matrix with components λ^+ (the larger eigenvalue) and λ^- (the smaller eigenvalue) in the notation of Kehr *et al*. [18], i.e.,

$$\boldsymbol{\lambda} = \begin{pmatrix} \lambda^+ & 0 \\ 0 & \lambda^- \end{pmatrix}$$

The flux equation (22) can then be rewritten as

$$\mathbf{E}^{-1}\mathbf{J} = -\boldsymbol{\lambda}\mathbf{E}^{-1}\nabla\mathbf{C}. \tag{24}$$

The eigenvalue λ^-, which describes the rate with which gradients in the concentration of A and B atoms dissipate by an intermixing mode is the most rigorous formulation of what is commonly referred to as an *interdiffusion* coefficient.

4. Cluster Expansion

The Green–Kubo expressions for diffusion coefficients are proportional to the ensemble averages of the square of the collective distance travelled by the diffusing particles of the solid. Trajectories of interacting diffusing particles can be obtained with kinetic Monte Carlo simulations in which particles migrate on a crystalline network with migration rates given by Eq. (1). The migration rates of a specific atom, however, depend on the local arrangement of the other diffusing atoms through the configuration dependence of the activation barrier and frequency prefactor. Ideally, the activation barrier for each local environment could be calculated from first-principles. Nevertheless, this is computationally impossible, as the number of configurations are exceedingly large, and first-principles activation barrier calculations have a high computational cost. It is here that the cluster expansion formalism [1–3] becomes invaluable as a tool to extrapolate energy values calculated for a few configurations to determine the energy for any arrangement of atoms in a crystalline solid.

In this section, we describe the cluster expansion formalism and how it can be applied to characterize the configuration dependence of the activation barrier for diffusion. We first focus on describing the configurational energy of atoms residing at their equilibrium sites, i.e., of the configurational energy of the end points of any hop.

4.1. General Formalism

We restrict ourselves to binary problems though the cluster expansion formalism is valid for systems with any number of species [1, 2]. While it is clear that two component alloys without crystalline defects such as vacancies are

binary problems, atoms residing on the interstitial sites of a host can be treated as a binary system as well, with the interstitial atoms constituting one of the components and the vacancies the other. In crystals, atoms can be assigned to well defined sites, even when relaxations from ideal crystallographic positions occur. There is always a one to one correspondence between each atom and a crystallographic site. If there are M crystallographic sites, then there are 2^M possible arrangements of two species over those sites. To characterize a particular configuration, it is useful to introduce occupation variables σ_i that are $+1$ (-1) if an A (B which could be an atom different from A or a vacancy) resides at site i. The vector $\vec{\sigma} = (\sigma_1, \sigma_2, \ldots, \sigma_i, \ldots, \sigma_M)$ then uniquely specifies a configuration. The use of $\vec{\sigma}$, however, is cumbersome and a more versatile way of uniquely characterizing configurations can be achieved with polynomials ϕ_α of occupation variables defined as [1]

$$\phi_\alpha(\vec{\sigma}) = \prod_{i \in \alpha} \sigma_i \tag{25}$$

where i are sites belonging to a cluster α of crystal sites. Typical examples of clusters are a nearest neighbor pair cluster, a next nearest neighbor pair cluster, a triplet cluster etc. Examples of clusters on a two dimensional triangular lattice are illustrated in Fig. 5. There are 2^M different clusters of sites and therefore 2^M cluster functions $\phi_\alpha(\vec{\sigma})$.

It can be shown [1] that the set of cluster functions $\phi_\alpha(\vec{\sigma})$ form a complete and orthonormal basis in configuration space with respect to the scalar product

$$\langle f, g \rangle = \frac{1}{2^M} \sum_{\vec{\sigma}} f(\vec{\sigma}) g(\vec{\sigma}) \tag{26}$$

where f and g are any scalar functions of configuration. The sum in Eq. (26) extends over all possible configurations of A and B atoms over the M sites of the crystal. Because of their completeness and orthonormality over the space of configurations, it is possible to expand any function of configuration $f(\vec{\sigma})$ as a linear combination of the cluster functions $\phi_\alpha(\vec{\sigma})$. In particular, the configurational energy (with atoms relaxed around the crystallographic positions of the crystal) can be written as

$$E(\vec{\sigma}) = E_o + \sum_{\alpha} V_\alpha \phi_\alpha(\vec{\sigma}) \tag{27}$$

where the sum extends over all clusters α over the M sites. The coefficients V_α are constants and formally follow from the scalar product of $E(\vec{\sigma})$ with the cluster function $\phi_\alpha(\vec{\sigma})$

$$V_\alpha = \langle E(\vec{\sigma}), \phi_\alpha(\vec{\sigma}) \rangle = \frac{1}{2^M} \sum_{\vec{\sigma}} E(\vec{\sigma}) \phi_\alpha(\vec{\sigma}). \tag{28}$$

E_o is the coefficient of the empty cluster $\phi_\mathrm{o} = 1$ and is the average of $E(\vec{\sigma})$ over all configurations. Equation (27) is referred to as a cluster expansion of

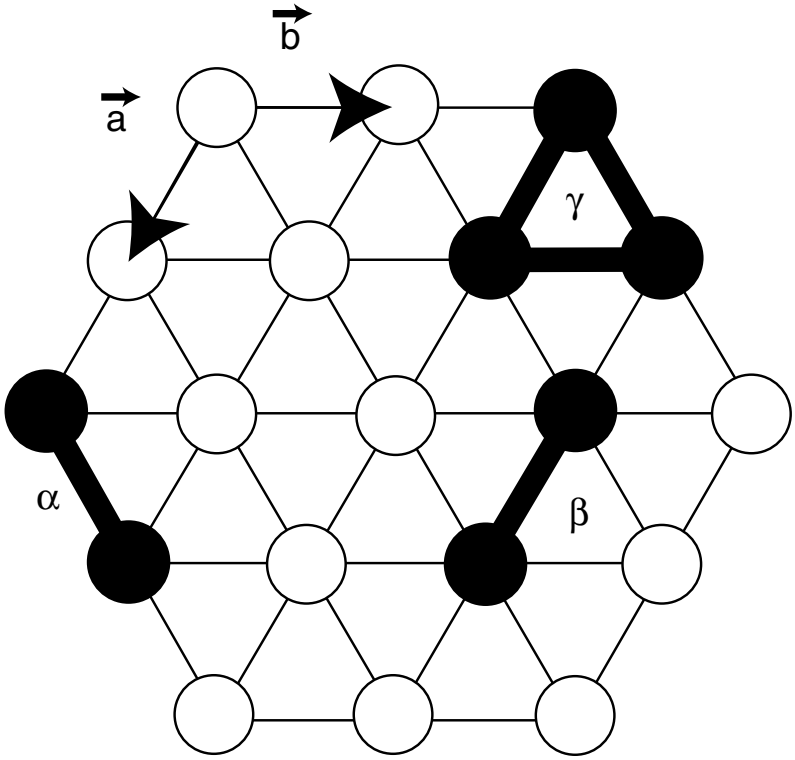

Figure 5. Examples of clusters for a two dimensional triangular lattice.

the configurational energy and the coefficients of the expansion V_α are called *effective cluster interactions* (ECI).

Equation (27) can be viewed as a generalized Ising model Hamiltonian containing not only nearest neighbor pair interactions, but also all other pair and multibody interactions extending beyond the nearest neighbors. Through Eq. (28), a formal link is made between the interaction parameters of the generalized Ising model and the configuration dependent ground state energies of the solid in each configuration $\vec{\sigma}$.

Clearly, the cluster expansion for the configurational energy, Eq. (27), is only useful if it converges rapidly, i.e., there exists a maximal cluster $\alpha_{\max}$ such that all ECI corresponding to clusters larger than $\alpha_{\max}$ can be neglected. In this case, the cluster expansion can be truncated to yield

$$E(\vec{\sigma}) = E_{\mathrm{o}} + \sum_{\alpha}^{\alpha_{\max}} V_\alpha \phi_\alpha(\vec{\sigma}) \tag{29}$$

A priori mathematical criteria for the convergence of the configurational energy cluster expansion do not exist. Experience indicates that convergence depends on the particular system being considered. In general, though, it can be expected that the lower order clusters extending over a limited range within the crystal will have the largest contribution in the cluster expansion.

4.2. Symmetry and the Cluster Expansion

Simplifications to the cluster expansion (27) or (29) can be made by taking the symmetry of the crystal into account [2]. Clusters are said to be equivalent by symmetry if they can be mapped onto each other with at least one space group symmetry operation. For example, clusters α and β of Fig. 5 are equivalent since a clockwise rotation of α by 60° followed by a translation by the vector $2\vec{b}$ maps α onto β. The ECI corresponding to clusters that are equivalent by symmetry have the same numerical value. In the case of α and β of Fig. 5, $V_\alpha = V_\beta$. All clusters that are equivalent by symmetry are said to belong to an orbit Ω_α where α is a representative cluster of the orbit. For any arrangement $\vec{\sigma}$ we can define averages over cluster functions $\phi_\alpha(\vec{\sigma})$ as

$$\langle \phi_\alpha(\vec{\sigma}) \rangle = \frac{1}{|\Omega_\alpha|} \sum_{\beta \in \Omega_\alpha} \phi_\beta(\vec{\sigma}) \tag{30}$$

where the sum extends over all clusters β belonging to the orbit Ω_α and $|\Omega_\alpha|$ represents the number of clusters that are symmetrically equivalent to α. The $\langle \phi_\alpha(\vec{\sigma}) \rangle$ are commonly referred to as correlation functions. Using the definition of the correlation functions and the fact that symmetrically equivalent clusters have the same ECI, we can rewrite the configurational energy normalized by the number of primitive unit cells N_p (i.e., number of Bravais lattice points of the crystal which is not necessarily equal to the number of crystal sites M), as

$$e(\vec{\sigma}) = \frac{E(\vec{\sigma})}{N_\mathrm{p}} = V_\mathrm{o} + \sum_\alpha m_\alpha V_\alpha \langle \phi_\alpha(\vec{\sigma}) \rangle \tag{31}$$

where m_α is the multiplicity of the cluster α, defined as the number of clusters per Bravais lattice point symmetrically equivalent with α (i.e., $m_\alpha = |\Omega_\alpha|/N_\mathrm{p}$) and $V_\mathrm{o} = E_\mathrm{o}/N_\mathrm{p}$. The sum in (31) is only performed over the symmetrically non-equivalent clusters.

4.3. Determination of the ECI

According to Eq. (28), the ECI for the energy cluster expansion are determined by the first-principles ground state energies for all the different

configurations $\vec{\sigma}$. Explicitly calculating the ECI according to the scalar product Eq. (28) is intractable. Techniques, such as direct configurational averaging (DCA), though, have been devised to approximate the scalar product (28) [2, 19, 20]. In recent years, the preferred method of obtaining ECI has been with an inversion method [21–29]. In this approach, energies $E(\vec{\sigma}_I)$ for a set of P periodic configurations $\vec{\sigma}_I$ with $I = 1, \ldots, P$ are calculated from first-principles and a truncated form of (31) is inverted such that it reproduces the $E(\vec{\sigma}_I)$ within a tolerable error when Eq. (31) is evaluated for configuration $\vec{\sigma}_I$. The simplest inversion scheme uses a least squares fit. More sophisticated algorithms involving linear programming techniques [30], cross-validation optimization [32] or the inclusion of k-space terms to account for long-range elastic strain have been developed [33, 34].

4.4. Local Cluster Expansion

The traditional cluster expansion formalism described so far is applicable to the configurational energy of the solid which is an extensive quantity. We will refer to these expansions as *extended cluster expansions*. Activation barriers, however, are equal to the difference between the energy of the solid when the migrating atom is at the activated state and that when the migrating atom is at the initial equilibrium site. Hence, the configuration dependence of the activation barrier of an atom needs to be described by a cluster expansion with no translational symmetry and as such it converges to a fixed value as the system size grows. Not only is the activation barrier a function of configuration, but it also depends on the direction of the hop. This is schematically illustrated in Fig. 6 in which the end points of the hop have a different configurational energy. Describing the configuration dependence of the activation barrier independent of the direction of the hop is straightforward if a *kinetically resolved* activation barrier is introduced [3], defined as

$$\Delta E_{\mathrm{KRA}} = E_{\mathrm{act}} - \frac{1}{n}\sum_{j=1}^{n} E_j \tag{32}$$

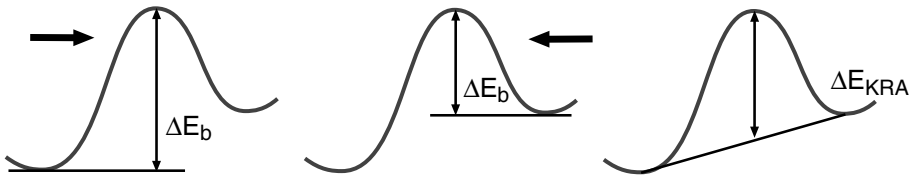

Figure 6. The activation barrier for migration depends on the direction of the hop when the energies of the end points of the hop are different.

where E_{act} is the energy of the solid with the migrating atom at the activated state and E_j are the energies of the solid with the migrating atom at the end points j of the hop. In most solids, there are n=2 end points to a hop, however, it is possible that more end points exist. All terms in Eq. (32) depend on the arrangement of atoms surrounding the end points of the hop and the activated state. The dependence of ΔE_{KRA} on configuration can, be described with a cluster expansion that has a point group symmetry compatible with the symmetry of the crystal as well as that of the activated state. For this reason, the cluster expansion of ΔE_{KRA} is called a *local* cluster expansion [3].

The kinetically resolved activation barrier is not the true activation barrier that enters in the transition state theory expression for the hop frequency, Eq. (1). It is merely a useful quantity that characterizes the configuration dependence of the activated state independent of the direction of the hop. The true activation barrier can be calculated from ΔE_{KRA} using

$$\Delta E_{\text{b}} = \left(\Delta E_{\text{KRA}} + \frac{1}{n} \sum_{j=1}^{n} E_j \right) - E_i \tag{33}$$

where E_i is the energy of the crystal with the migrating atom at the initial site of the hop. All quantities on the right hand side of Eq. (33) can be described with either a local cluster expansion (for ΔE_{KRA}) or an extended cluster expansion (for the configurational energy of the solid).

5. Practical Implementation

Calculating diffusion coefficients from first-principles in multicomponent solids involves three steps. First, a variety of *ab initio* energies for different atomic arrangements need to be calculated with an accurate first-principles method. This includes energies for a wide range of atomic arrangements over the sites of the crystal, as well as energies for migrating atoms placed at activated states surrounded by different arrangements. The latter calculations are typically performed with an atom at the activated state in large supercells. A useful technique to find the activated state between two equilibrium end points is the nudged elastic band method [31] which determines the lowest energy path between two equilibrium states. Calculating the vibrational prefactor requires a calculation of the phonon density of states for different atomic arrangements both with the migrating atom at its equilibrium site and at the activated state. While sophisticated techniques have been devised to characterize the configurational dependence of the vibrational free energy of a solid [35], for diffusion studies, a convenient simplification is the local harmonic approximation [36].

In the second step, the first-principles energy values for different atomic arrangements are used to determine the coefficients of both a local cluster expansion (for the kinetically resolved activation barriers) and a traditional extended cluster expansion (for the energy of the crystal with all atoms at non-activated crystallographic sites) with either a least squares fit or with one of the more sophisticated methods alluded to above. The cluster expansions enable the calculation of the energy and activation barrier for any arrangement of atoms on the crystal. They serve as a convenient and robust tool to extrapolate accurate first-principles energies calculated for a few configurations to the energy of any configuration. Hence the migration rates of Eq. (1) can be calculated for any arrangement of atoms.

The final step is the combination of the cluster expansions with kinetic Monte Carlo simulations to calculate the quantities entering the Green–Kubo expressions for the diffusion coefficients. Kinetic Monte Carlo simulations have been discussed extensively elsewhere [3, 37, 38]. Applied to diffusion in crystals, kinetic Monte Carlo algorithms are used to simulate the stochastic migrations of many atoms, hopping to neighboring sites with frequencies given by Eq. (1). A kinetic Monte Carlo simulation starts from a representative arrangement of atoms (typically obtained with a standard Monte Carlo method for lattice models). As atoms migrate, their trajectories and the time are kept track of, enabling the calculation of the quantities between the brackets in the Green–Kubo expressions. Since the Green–Kubo expressions involve ensemble averages, many kinetic Monte Carlo runs which start from different representative initial conditions are necessary. Depending on the desired accuracy, averages need to be performed over the trajectories departing from between 100 and 10 000 different initial conditions.

6. Examples

Two examples of first-principles calculations of diffusion coefficients in multi-component solids are reviewed in this section. The first is for lithium diffusion in Li_xCoO_2 and is an example of nondilute interstitial diffusion. The second example, diffusion in the fcc based Al–Li alloy, corresponds to a substitutional system.

6.1. Interstitial Diffusion

Li_xCoO_2 consists of a host structure made up of a CoO_2 frame work. Layers of interstitial sites that can be occupied by lithium ions reside between O–Co–O slabs. The interstitial sites are octahedrally coordinated by oxygen and they form two dimensional triangular lattices. As described in Section 2.1,

two migration mechanisms exist for lithium: a single vacancy mechanism whereby lithium squeezes through a dumbell of oxygen atoms into an isolated vacancy and a divacancy mechanism in which lithium migrates through an adjacent tetrahedral site into a vacant site that is part of a divacancy [3]. The two migration mechanisms are illustrated in Fig. 1.

Not only does the local arrangement of lithium ions around a hopping ion determine the migration mechanism, it also affects the value of the activation barrier for a particular migration mechanism. Figure 7 illustrates kinetically resolved activation barriers calculated from first- principles (LDA) for a variety of different lithium-vacancy arrangements around the migrating ion at different bulk lithium concentrations [3]. Note that for a given bulk composition, many possible lithium-vacancy arrangements around an atom in the activated state exist. The kinetically resolved activation barriers illustrated in Fig. 7 correspond to only a small subset of the these many configurations. The local cluster expansion is used to extrapolate from this set to all the configurations needed in a kinetic Monte Carlo simulation.

Figure 7 shows that the activation barrier for the divacancy migration mechanism can vary by more that 200 meV with lithium concentration. The increase in activation barrier upon lithium removal from the host can be traced to the contraction of the host along the c-axis as the lithium concentration is reduced [3].

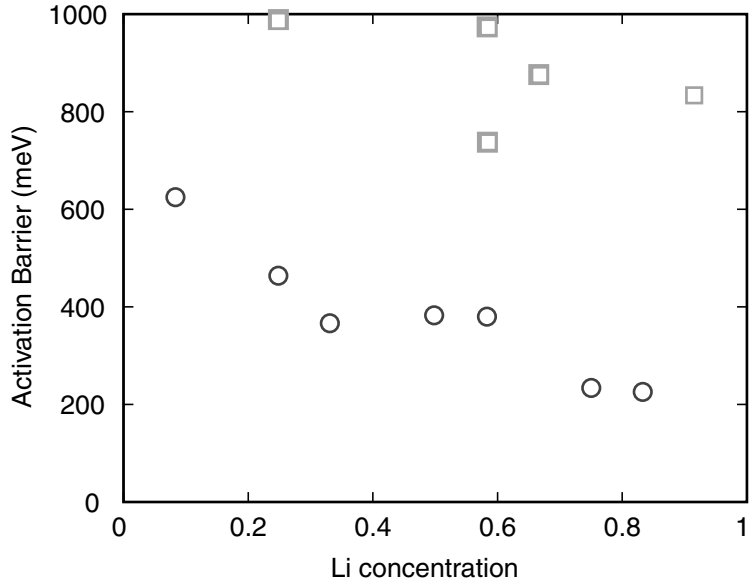

Figure 7. A sample of first-principles (LDA) kinetically resolved activation barriers ΔE_{KRA} for the divacancy hop mechanism (circles) and the single vacancy mechanism (squares).

This contraction disporportionately penalizes the activated state over the end point states of the divacancy hop mechanism. Another contribution to the variation in activation barrier with composition derives from the fact that the activated state is very close in proximity to a Co ion, which becomes progressively more oxidized (i.e., its eff ective charge becomes more positive) as the overall lithium concentration is reduced [3, 29]. This leads to an increase in the electrostatic repulsion between the activated Li and the Co as x is reduced.

Extended and local cluster expansions can be constructed to describe both the configurational energy of Li_xCoO_2 and the configuration dependence of the kinetically resolved activation barriers. An extended cluster expansion for the first-principles configurational energy of Li_xCoO_2 has been described in detail in Ref. [29]. This cluster expansion when combined with Monte Carlo simulations accurately predicts phase stability in Li_xCoO_2. In particular, two ordered lithium-vacancy phases are predicted at $x = 1/2$ and $x = 1/3$. Both phases are observed experimentally [39, 40]. A local cluster expansion for the kinetically resolved activation barriers has been described in Ref [3].

Figure 8 illustrates calculated diffusion coefficients at 300 K determined by applying kinetic Monte Carlo simulations to the cluster expansions of Li_xCoO_2 [3]. While the configuration dependence of the activation barriers were rigorously accounted for with the cluster expansions, no attempt in these calculations was made to describe the migration rate prefactor ν^* from first- principles. Instead, a value of 10^{13} Hz was used for all compositions and environments. Figure 8(a) shows both D_J and the chemical diffusion coefficient D, while Fig. 8(b) illustrates the thermodynamic factor F, which was determined by calculating fluctuations in the number of lithium particles in grand canonical Monte Carlo simulations [3] (see Section 3.1). Notice that the calculated diffusion coefficient varies by several orders of magnitude with composition, showing that the assumption of a concentration independent diffusion coefficient in this system is unjustified. The thermodynamic factor F is a measure for the deviation from ideality. In the dilute limit ($x \to 0$), interactions between lithium ions are negligible and the configurational thermodynamics approximates that of an ideal solution. In this limit the thermodynamic factor is 1. As x increases from 0, and the solid departs from ideal behavior, the thermodynamic factor increases substantially.

The local minima in D_J and D at $x = 1/2$ and $x = 1/3$ are a result of lithium ordering at those compositions. Lithium-vacancy ordering effectively locks in lithium ions into energetically favorable sublattice positions which reduces ionic mobility. The thermodynamic factor on the other hand exhibits peaks at $x = 1/2$ and $x = 1/3$ as the configurational thermodynamics of an ordered phase deviates strongly from ideal behavior. The peak signifies the fact that in an ordered phase, a small gradient in composition leads to an enormous gradient in chemical potential, and hence a large thermodynamic driving force for diffusion. This partly compensates the reduction in D_J.

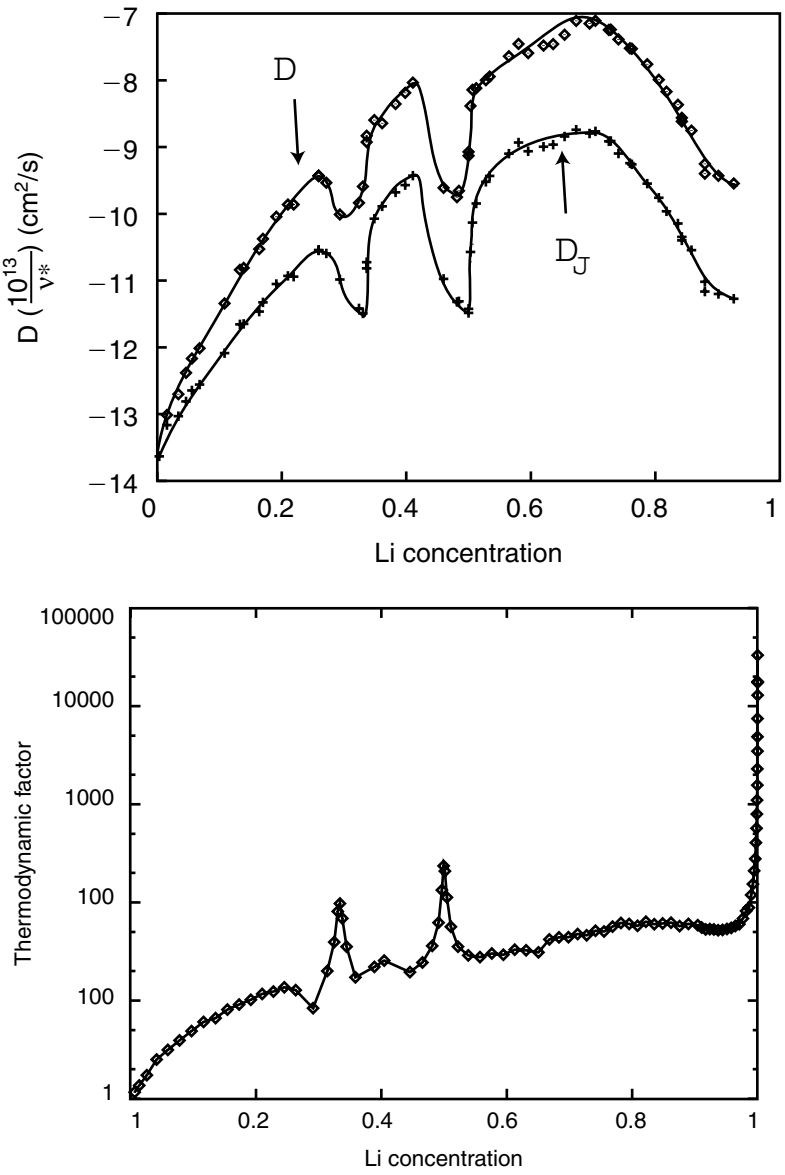

Figure 8. (a) Calculated self diffusion coefficient D_J and chemical diffusion coefficient D for Li_xCoO_2 at 300 K. (b) The thermodynamic factor of Li_xCoO_2 at 300 K.

A similar computational approach can be followed to determine for example the diffusion coefficient for oxygen diffusion on a platinum (111) surface. If in addition to oxygen, sulfur atoms are also adsorbed on the platinum surface, Green–Kubo relations for binary interstitial diffusion would be needed. Furthermore, ternary cluster expansions are then necessary to describe the configuration dependence of the energy and kinetically resolved activation barrier as there are then three species: oxygen, sulfur and vacancies.

6.2. Substitutional Diffusion

To illustrate diffusion in a binary substitutional solid, we consider the fcc Al–Li alloy. While $Al_{1-x}Li_x$ is predominantly stable in the bcc based crystal structure, it is metastable in fcc up to $x = 0.25$. In fact, it is the metastable form of fcc $Al_{1-x}Li_x$ that strengthens the important candidate alloy for aerospace applications.

A first step in determining the diffusion coefficients in this system is an accurate first-principles characterization of the alloy thermodynamics. This can be done with a binary cluster expansion for the configurational energy [26]. The expansion coefficients of the cluster expansion were fit to the first-principles energies (LDA) of more than 70 different periodic lithium-aluminum arrangements on the fcc lattice [41]. Figure 9(a) illustrates the calculated metastable fcc based phase diagram of $Al_{1-x}Li_x$ obtained by applying Monte Carlo simulations to the cluster expansion [41]. The phase diagram shows that a solid solution phase is stable at low lithium concentration and at high temperature. At $x = 0.25$, the $L1_2$ ordered phase is stable. In this ordered phase the Li atoms occupy the corner points of the conventional cubic fcc unit cell.

Diffusion in most metals is dominated by a vacancy mechanism. Hence it is not sufficient to simply characterize the thermodynamics of the strictly binary Al–Li alloy. Real alloys always have a dilute concentration of vacancies that wander through the crystal and in the process redistribute the atoms of the solid. The vacancies themselves have a thermodynamic preference for particular local environments over others which in turn affects the mobility of the vacancies. Treating vacancies in addition to Al and Li makes the problem a ternary one and in principles would require a ternary cluster expansion. Nevertheless, since vacancies are present in dilute concentrations, a ternary cluster expansion can be avoided by using a local cluster expansion to describe the configuration dependence of the vacancy formation energy [41]. In effect, the local cluster expansion serves as a perturbation to the binary cluster expansion to describe the interaction of a dilute concentration of a third component, in this case the vacancy. A local cluster expansion for the vacancy formation energy in fcc Al–Li was constructed by fitting to first-principles (LDA) vacancy formation energies in 23 different Al–Li arrangements [41]. Combining the vacancy

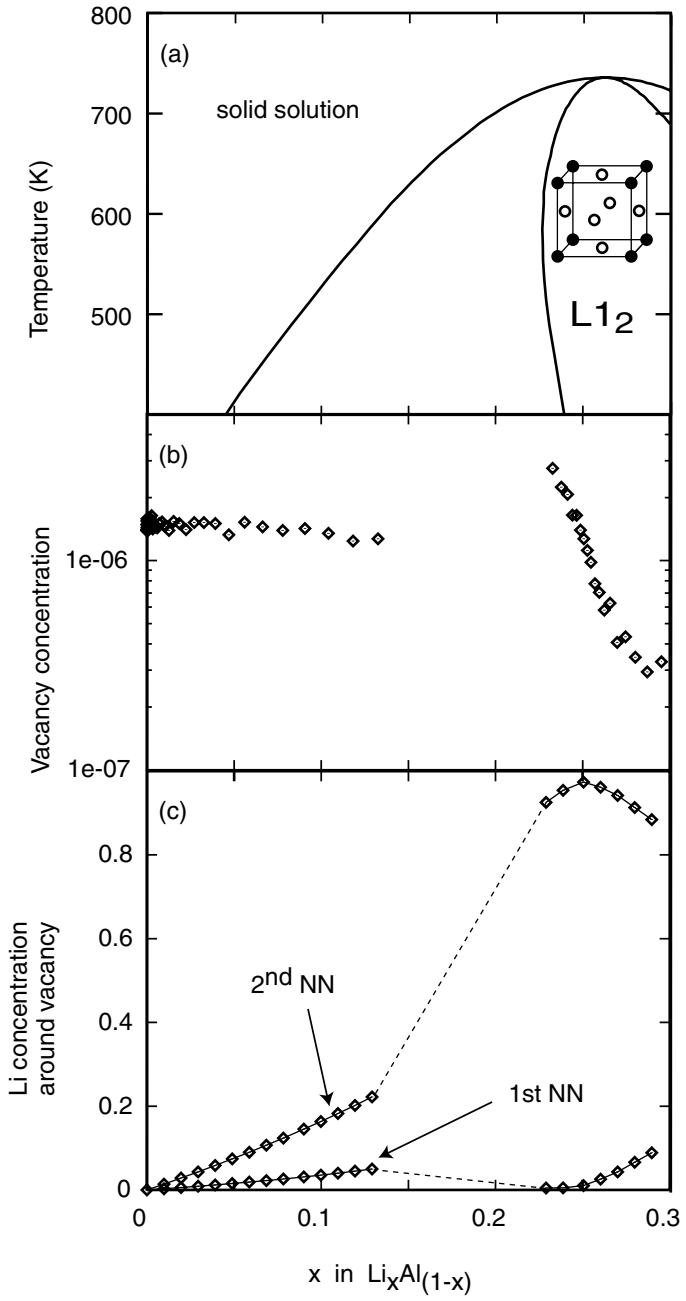

Figure 9. (a) First-principles calculated phase diagram of fcc based $Al_{(1-x)}Li_x$ alloy. (b) Calculated equilibrium vacancy concentration as a function of bulk alloy composition at 600 K. (c) Average lithium concentration in the first two nearest neighbor shells around a vacancy. The dashed line corresponds to the average bulk lithium concentration.

formation local cluster expansion with the binary cluster expansion for Al–Li in Monte Carlo simulations enables a calculation of the equilibrium vacancy concentration as a function of alloy composition and temperature. Figure 9(b) illustrates the result for Al–Li at 600 K [41]. While the vacancy concentration is more or less constant in the solid solution phase, it can vary by an order of magnitude over a small concentration range in the ordered $L1_2$ phase at 600 K.

Another relevant thermodynamic property that is of importance for diffusion is the equilibrium short range order around a vacancy in fcc Al–Li. Monte Carlo simulations using the cluster expansions predict that the vacancy repels lithium ions, preferring a nearest neighbor shell rich in aluminum. Illustrated in Fig. 9(c) is the lithium concentration in shells with varying distance around a vacancy. The lithium concentration in the first nearest neighbor shell is less than the bulk alloy composition, while it is slightly higher than the bulk composition in the second nearest neighbor shell. This indicates that the vacancy repels Li and attracts Al. In the ordered phase, stable at 600 K between $x = 0.23$ and 0.3, the degree of order around the vacancy is even more pronounced as illustrated in Fig. 9(c). Between $x = 0.23$ and 0.3, the vacancy is predominantly surrounded by Al in its first and third nearest neighbor shells and by Li in its second and fourth nearest neighbor shells. This corresponds to a situation in which the vacancy occupies the lithium sublattice of the $L1_2$ ordered phase. Clearly the thermodynamic preference of the vacancies for a specific local environment will have an impact on their mobility through the crystal.

While thermodynamic equilibrium determines the degree of order within the alloy and which environments the vacancies are attracted to, atomic migration mediated by a vacancy mechanism involves passing through activated states, which requires passing over an energy barrier that also depends on the local degree of order. Contrary to what is predicted for Li_xCoO_2, the kinetically resolved activation barriers in fcc $Al_{1-x}Li_x$ are not very sensitive to configuration and bulk composition [42]. For each type of atom (Al or Li), the variations in kinetically resolved activation barriers are within the numerical errors of the first-principles method (50 meV for a plane wave pseudopotential method using 107 atom supercells). This is likely the result of a negligible variation in volume of fcc $Al_{1-x}Li_x$ with composition. But while the migration barriers do not depend significantly on configuration, they are very different depending on which atom performs the hop. The first-principles calculated migration barrier for Al hops are systematically between 150 to 200 meV larger than for Li hops [42].

The thermodynamic tendency of the vacancy to repel lithium atoms deprives Li of diffusion mediating defects. Kinetically, though, Li has a lower activation barrier relative to Al for migration into an adjacent vacancy. Hence a trade-off exists between thermodynamics and kinetics. While Li exchanges more readily with a neighboring vacancy, thermodynamically it has less access to those vacancies. Quantitatively determining the effect of this trade-off requires explicit

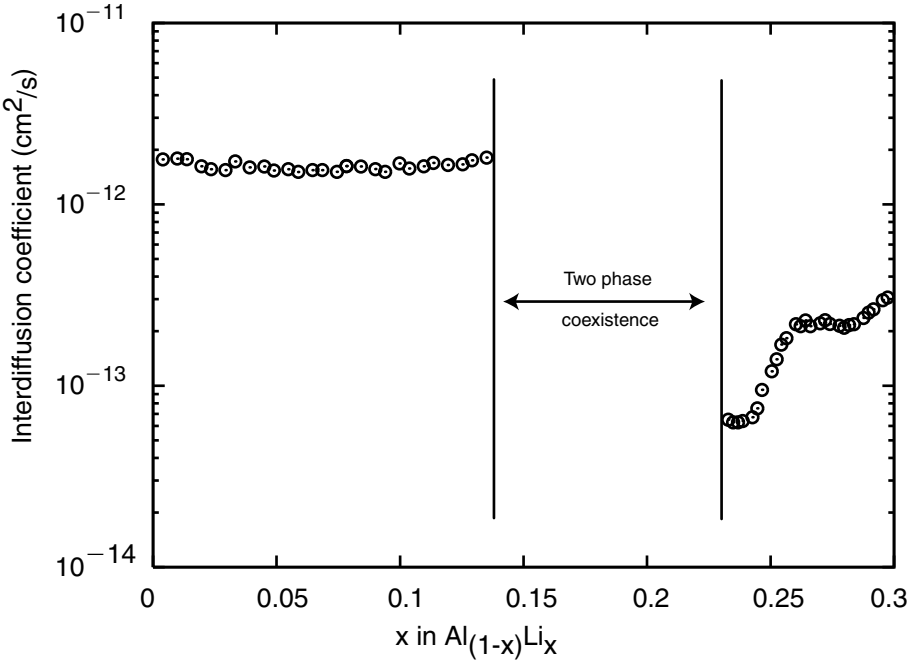

Figure 10. Calculated interdiffusion coefficient (the λ^- eigenvalue of the 2×2 **D** matrix) for fcc $Al_{(1-x)}Li_x$ alloy at 600 K.

evaluation of diffusion coefficients. This can be done by applying kinetic Monte Carlo simulations to cluster expansions that describe the configurational energy and kinetically resolved activation barriers for Al, Li and dilute vacancies on the fcc lattice. Figure 10 illustrates the calculated interdiffusion coefficient at 600 K obtained by diagonalizing the **D** matrix of Eq. (14) [42]. The coefficient for interdiffusion describes the rate with which the Al and Li atoms intermix in the presence of a concentration gradient in the two species. The calculated interdiffusion coefficient is more or less constant in the solid solution phase, but drops by more than an order of magnitude in the $L1_2$ ordered phase. The thermodynamic preference of the vacancies for the lithium sublattice sites of $L1_2$ dramatically constricts the trajectory of the vacancies, leading to a drop in overall mobility of Li and Al.

7. Conclusion

In this chapter, we have presented the statistical mechanical formalism that relates phenomenological diffusion coefficients for multicomponent solids to microscopic fluctuations of the solid at equilibrium. We have focussed on

diffusion that is mediated by a vacancy mechanism and have distinguished between interstitial systems and substitional systems. An important property of multicomponent solids is the existence of configurational disorder among the constituent species. This adds a level of complexity in calculating diffusion coefficients from first- principles since the activation barriers vary along an atom's trajectory as a result of variations in the local degree of atomic order. In this respect, the cluster expansion is an invaluable tool to describe the dependence of the energy, in particular of the activation barrier, on atomic configuration. While the formalism of calculating diffusion coefficients from first-principles in multicomponent solids has been established, many opportunities exist to apply it to a wide variety of multicomponent crystalline solids, including metals, ceramics and semiconductors. Faster computers and improvements to electronic structure methods that go beyond density functional theory will lead to more accurate first-principles approximations to activation barriers and vibrational prefactors. It is only a matter of time before first-principles diffusion coefficients for multicomponent solids are routinely used in continuum simulations of diffusional phase transformations and electrochemical devices such as batteries and fuel cells.

Acknowledgments

We acknowledge support from the AFOSR, grant F49620-99-1-0272 and the Department of Energy, Office of Basic Energy Sciences under Contract No. DE-FG02-96ER45571. Additional support came from NSF (ACI-9619020) through computing resources provided by NPACI at the San Diego Supercomputer Center.

References

[1] J.M. Sanchez, F. Ducastelle, and D. Gratias, *Physica A*, 128, 334, 1984.
[2] D. de Fontaine, In: H. Ehrenreich and D. Turnbull (eds.), *Solid State Physics.*, Academic Press, New York, pp. 33, 1994.
[3] A. Van der Ven, G. Ceder, M. Asta, and P.D. Tepesch, *Phys. Rev. B*, 64, 184307, 2001.
[4] S.R. de Groot and P. Mazur, *Non-Equilibrium Thermodynamics*, Dover Publications, Mineola, NY, 1984.
[5] G.H. Vineyard, *J. Phys. Chem. Solids*, 3, 121, 1957.
[6] D. Chandler, *Introduction to Modern Statistical Mechanics*, Oxford University Press, Oxford, 1987.
[7] R. Zwanzig, *Annu. Rev. Phys. Chem.*, 16, 67, 1965.
[8] R. Zwanzig, *J. Chem. Phys.*, 40, 2527, 1964.
[9] Y. Zhou and G.H. Miller, *J. Phys. Chem.*, 100, 5516, 1996.
[10] R. Gomer, *Rep. Prog. Phys.*, 53, 917, 1990.

[11] M. Tringides and R. Gomer, *Surf. Sci.*, 145, 121, 1984.
[12] C. Uebing and R. Gomer, *J. Chem. Phys.*, 95, 7626, 1991.
[13] A.R. Allnatt, *J. Chem. Phys.*, 43, 1855, 1965.
[14] A.R. Allnatt, *J. Phys. C: Solid State Phys.*, 15, 5605, 1982.
[15] R.E. Howard and A.B. Lidiard, *Rep. Prog. Phys.*, 27, 161, 1964.
[16] A.R. Allnatt and A.B. Lidiard, *Rep. Prog. Phys.*, 50, 373, 1987.
[17] J.W. Cahn and F.C. Larche, *Scripta Met.*, 17, 927, 1983.
[18] K.W. Kehr, K. Binder, and S.M. Reulein, *Phys. Rev. B*, 39, 4891, 1989.
[19] C. Wolverton, G. Ceder, D. de Fontaine, and H. Dreysse, *Phys. Rev. B*, 45, 13105, 1992.
[20] C. Wolverton and A. Zunger, *Phys. Rev. B*, 50, 10548, 1994.
[21] J.W.D. Connolly and A.R. Williams, *Phys. Rev. B*, 27, 5169, 1983.
[22] J.M. Sanchez, J.P. Stark, and V.L. Moruzzi, *Phys. Rev. B*, 44, 5411, 1991.
[23] Z.W. Lu, S.H. Wei, A. Zunger, S. Frotapessoa, and L.G. Ferreira, *Phys. Rev. B*, 44, 512, 1991.
[24] M. Asta, D. de Fontaine, M. Vanschilfgaarde, M. Sluiter, and M. Methfessel, *Phys. Rev. B*, 46, 5055, 1992.
[25] M. Asta, R. McCormack, and D. de Fontaine, *Phys. Rev. B*, 48, 748, 1993.
[26] M.H.F. Sluiter, Y. Watanabe, D. de Fontaine, and Y. Kazazoe, *Phys. Rev. B*, 53, 6136, 1996.
[27] P.D. Tepesch, *et al.*, *J. Am. Cer. Soc.*, 79, 2033, 1996.
[28] V. Ozolins, C. Wolverton, and A. Zunger, *Phys. Rev. B*, 57, 6427, 1998.
[29] A. Van der Ven, M.K. Aydinol, G. Ceder, G. Kresse, and J. Hafner, *Phys. Rev. B*, 58, 2975, 1998.
[30] G.D. Garbulsky and G. Ceder, *Phys. Rev. B*, 51, 67, 1995.
[31] G. Mills, H. Jonsson, and G.K. Schenter, *Surf. Sci.*, 324, 305, 1995.
[32] A. van de Walle and G. Ceder, *J. Phase Eqilib.*, 23, 348, 2002.
[33] D.B. Laks, L.G. Ferreira, S. Froyen, and A. Zunger, *Phys. Rev. B*, 46, 12587, 1992.
[34] C. Wolverton, *Philos. Mag. Lett.*, 79, 683, 1999.
[35] A. van de Walle and G. Ceder, *Rev. Mod. Phys.*, 74, 11, 2002.
[36] R. LeSar, R. Najafabadi, and D.J. Srolovitz, *Phys. Rev. Lett.*, 63, 624, 1989.
[37] A.B. Bortz, M.H. Kalos, and J.L. Lebowitz, *J. Comput. Phys.*, 17, 10, 1975.
[38] F.M. Bulnes, V.D. Pereyra, and J.L. Riccardo, *Phys. Rev. E*, 58, 86, 1998.
[39] J.N. Reimers and J.R. Dahn, *J. Electrochem. Soc.*, 139, 2091, 1992.
[40] Y. Shao-Horn, S. Levasseur, F. Weill, and C. Delmas, *J. Electrochem. Soc.*, 150, A366, 2003.
[41] A. Van der Ven and G. Ceder, *Phys. Rev. B.*, 2005 (in press).
[42] A. Van der Ven and G. Ceder, *Phys. Rev. Lett.*, 2005 (in press).